

UV and an IR Lasers Pumped by Generators with Inductive Energy Storage

A.N. Panchenko, V.F. Tarasenko, and A.E. Tel'minov

*Institute of High-Current Electronics SB RAS, 2/3, Akademichesky ave., Tomsk, 634055, Russia
Phone: 8(3822) 49-23-92, Fax: 8(3822) 49-24-10, E-mail: alexei@loi.hcei.tsc.ru*

Abstract – Laser and discharge parameters in mixtures of rare gases with halogens driven by a pre-pulse-sustainer circuit technique are studied. Inductive energy storage (IES) with semiconductor opening switch was used for the high-voltage pre-pulse formation. It was shown that the pre-pulse with a high amplitude and short rise-time along with sharp increase of discharge current allow to form long-lived stable discharge different gas mixtures. Improve of both pulse duration and output energy was achieved for XeCl-, XeF-, and KrF excimer lasers. Maximal at that date radiation power, output energy and laser pulse duration were obtained in N₂-NF₃ (SF₆) and He-F₂ (NF₃) gas mixtures, as well.

1. Introduction

Development of efficient discharge lasers on different gas mixtures is associated with the solution of the following two problems. First problem consists in formation and sustaining of uniform volume discharge in halogen containing gas mixtures. Second one is improvement of the efficiency of a stored energy transfer from a pumping generator to this volume discharge plasma. Volume discharge is formed using different preionization sources (UV radiation, x-rays, electron beam, and so on) and over-voltage applied to a laser gap.

Comprehensive double discharge pumping circuits based on spark switches or saturable inductors are used for efficient energy transfer to the discharge plasma [1, 2]. In these circuits, a high-voltage pre-pulse generator with low stored energy ignites volume discharge while a low-voltage storage deposits main part of pumping energy in the impedance matched mode. This pumping technique based on PFL allowed developing long-pulse XeCl discharge lasers with efficiency up to 4–5% [1]. However, application of the double discharge circuits for lasers on gas mixtures with F₂ or NF₃ (XeF, KrF, and ArF and other lasers) was limited due to fast discharge collapse [2, 3].

Early we suggested alternative way of the pre-pulse formation using an inductive energy storage for the pre-pulse formation [4–6]. In this method, part of energy stored in a primary capacitor is transferred into circuit inductor of the pumping generator and than to the load using special device named opening switch.

The present paper reports operation of the IES-generators with semiconductor opening switch on gas

discharge load. Output laser parameters obtained with the generators are presented, as well.

2. INE generator design and measurement procedure

Several laser devices were used in experiments. Their circuit diagram is shown in Fig.1. Discharge cross-section and active length of lasers No. 1 and No. 2 with spark UV preionization were $S = (0.5-2) \cdot 4 \text{ cm}^2$ and $l = 72$ and 90 cm , respectively. The discharge gap was $d = 4 \text{ cm}$. The pumping generator consisted of storage $C_0 = 38$ or 70 (No. 1), 160 nF (No. 2) and peaking $C_1 = 2.45 \text{ nF}$ (No. 1) or 3.3 nF (No. 2) capacitors. Wide-aperture laser No. 3 with active volume $V = 6 \text{ l}$ and X-ray preionisation was equipped with $C_0 = 45 \text{ nF}$ and $C_1 = 4.5-8.5 \text{ nF}$ [7].

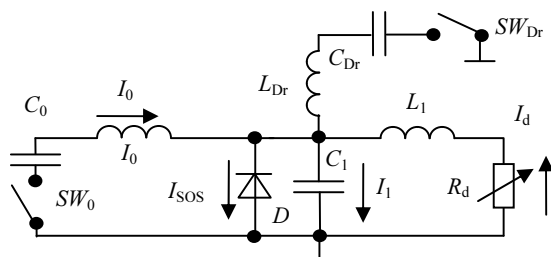


Fig. 1. Circuit diagram of the laser with IES generator. SW_0 , SW_{Dr} – spark gaps; C_0 – storage capacitor; C_1 – peaking capacitors; C_{Dr} – driving capacitor of SOS – diodes D ; L_0 , L_1 , L_{Dr} – circuit inductors, R_d – discharge resistance, I_i – currents in different circuits

Semiconductor opening switch consists of 10 SOS-diodes placed in parallel with the peaking capacitors. Maximal opening current of the SOS diode was measured to be as high as 4 kA, the response time is 10–20 ns. To run the diodes as current interrupters, a current of 100–500 A was passed through each diode in the forward direction during 500 ns from a driving capacitor $C_{Dr} = 10 \text{ nF}$ charged to the voltage $U_1 = 10-35 \text{ kV}$ and triggered by the spark gap SW_{Dr} . Therewith the driving energy can be as low as 1 J.

The pumping generator of each laser can operate as conventional LC-circuit. In this case, the capacitor C_{Dr} is not charged.

Discharge and laser parameters were studied in gas mixtures of Ne, Xe, Kr with HCl, F₂, NF₃, N₂ with NF₃ or SF₆ and He with F₂ and NF₃ at total gas pressure up to 3.5 atm.

Optical cavity was formed by totally reflecting Al mirror and dielectric mirrors with reflectivity 30–80% at $\lambda = 222\text{--}1050\text{ nm}$ or uncoated quartz plate.

The laser output energy was measured using an OPHIR calorimeter with FL-250A or PE-50BB sensors. The laser pulse waveforms were measured in the far zone with FEK-22 or FEK-29 vacuum photodiodes. The laser spectra were recorded using a Stellar-Net EPP2000-C25 spectrometer or MDR-12 monochromator.

In the experiments, we measured current through the laser gap I_d , current in the C_0 circuit I_0 , C_1 capacitor current I_1 , SOS-diode current I_{SOS} with Rogovsky coils and voltage across the laser gap U_d and diodes U with voltage dividers. Electrical signals were recorded with a TDS – 3034 digital oscilloscope.

3. Operation of the IES generator on a gas discharge load

Comparison of operation of the IES- and LC- pumping generators is shown in Fig. 2. Stage of the direct pumping of SOS-diodes is not shown. Inverse current begins to pass through the opening switch from the storage capacitor C_0 after spark gap SW_0 closing. In $\sim 30\text{ ns}$ resistance of SOS-diodes sharply increases, and current through the diodes is interrupted. During this time part of energy $E_L = L_0 I_{2open}^2 / 2$, where I_{open} is the opening current, is transferred into the circuit inductance L_0 . For the case shown in Fig. 2, $I_{open} = 20\text{ kA}$ and $E_L = 5\text{ J}$. Then the IES and C_0 sharply charges the peaking capacitors up to 40–80 kV within 20–30 ns, and a high-voltage pre-pulse across the laser gap is formed. After the laser gap breakdown residual IES current I_0 is added with the discharge current of peaking capacitors I_1 providing current spike in the laser gap and formed short powerful pumping pulse. Joint action such factors as high breakdown voltage and sharp increase of the discharge current improve discharge uniformity and allows forming long-lived volume discharge in gas mixtures with halogens [5]. Than energy stored in C_0 is deposited into the load during $\sim 150\text{--}200\text{ ns}$.

In the case of the LC-generator, peaking capacitors are charged only from C_0 , and the rate of the voltage increase is slowed down. Therewith breakdown voltage and amplitude of the first discharge current spike decrease by a factor of 1.5–2. By the end of half-period of the I_0 current voltage across the diodes changes its sign, and current through the opening switch begins to pass again. This means that in the case of mismatching between the pulsed generator impedance and discharge resistance at high U_0 subsequent current oscillations will pass through the diodes. This reduces erosion of the electrode surface and improves reliability of the laser operation under excitation by generators with SOS-diodes. Duration of discharge current I_d is longer than the half-period of I_0 due to discharge of inductance L_1 through diodes and the laser gap.

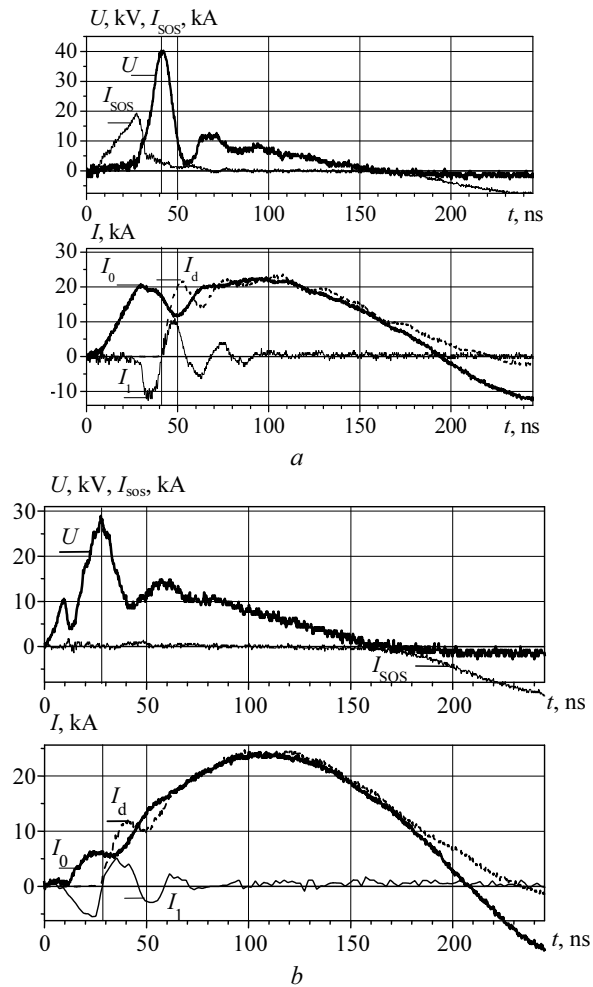


Fig. 2. Waveforms of voltage across SOS-diodes and C_1 (U), SOS-diode current (I_{SOS}), current in the laser gap (I_d) and currents in the circuit of storage (I_0) and peaking (I_1) capacitors in the case of the IES (a) and LC (b) generators obtained in N_2 at $p = 78\text{ Torr}$. Laser No. 1, $C_0 = 70\text{ nF}$, $U_0 = 30\text{ kV}$, $U_1 = 25\text{ kV}$

4. Experimental results and discussion

Nitrogen laser. UV lasing on first (electron bands $B^3\Pi_g - A^3\Sigma_u^+$) and second positive system ($C^3\Pi_u - B^3\Pi_g$) of N_2 can be obtained only at high electric field strength across the laser gap $E/p > 100\text{ V/cm} \cdot \text{Torr}$. Therewith under transverse discharge excitation from LC-generators voltage across the laser gap collapses during few nanoseconds and the laser pulse duration is as usual no longer than $\sim 10\text{ ns}$. Additions of electronegative admixtures, such as NF_3 and SF_6 into N_2 can slow-down the voltage drop rate due to increase of the electron attachment coefficient and slightly expand the laser pulse duration. Maximal laser output on the UV transition 0–0 ($\lambda = 337.1\text{ nm}$) was 40 mJ [8], while that on the IR lines did not exceed 5 mJ [9] using LC-generators.

Optimization of excitation mode from the IES generator allows to improve the output energy in the

UV and IR ranges and expand the laser pulse at $\lambda = 337.1$ nm (see Fig. 3). In our experiments, maximal UV laser output was as high as 50 mJ, while that on the IR transition exceeds 20 mJ. Lasing at 337.1 nm began within 40 ns earlier the IR pulse and was about 40 ns in duration (FWHM). Therewith weak UV laser action was observed during the IR pulse. Level $B^3\Pi_g$ is lower for the UV-transition. At the same time, it is upper level for the IR-transition. This means that intense IR lasing strongly depopulates $B^3\Pi_g$ state and can maintain population inversion on the $C^3\Pi_u - B^3\Pi_g$ transition. Therewith the UV laser pulse duration on the base was as long as 100 ns.

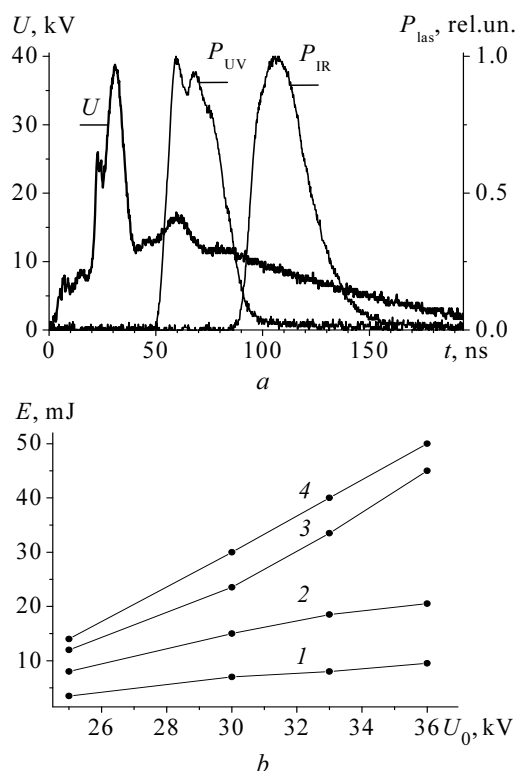


Fig. 3. Waveforms of the voltage across the laser gap U and UV (P_{UV}) and IR (P_{IR}) laser pulses in the $N_2:SF_6 = 30:3$ Torr mixture at $U_0 = 33$ kV (a); laser energy at 337.1 nm (1, 3, 4) and IR transitions (2) in pure N_2 at 60 Torr (1) and with 1.5 Torr (2) and 7.5 Torr (3) SF_6 and in the $N_2:SF_6 = 30:9$ Torr mixture (b) as function of U_0 . Laser No. 2

In the case of the laser No. 3 with active volume output energy of UV nitrogen laser exceeds 100 mJ with peak power of 6 mW [7].

Laser on FI transitions. Usually severe arcing is observed within several tens of ns in mixtures of fluorine with helium under transverse discharge excitation, and therefore the lasing lasts only 10–20 ns [10, 11]. The use of the IES allows to form stable volume discharge in the He- F_2 mixtures with duration about 100–150 ns. As a result, the FI-laser pulse duration was about 100 ns. Peak laser power was over 400 kW. Maximal output on the FI lines in mixtures with F_2 was about 8 mJ. The parameters obtained are maximal

at the date for FI laser excited by a transverse discharge.

XeF laser. Fig. 4 depicts waveforms of the voltage across the laser gap, XeF laser pulse and discharge view in different pumping modes. Slow increase of the voltage pulse and low breakdown voltage is typical for pumping by the LC-generator. As a result, violation of discharge uniformity is observed. The IES increase both the rate of the voltage rise and breakdown voltage by a factor of ~ 1.5 . Improvement of discharge stability results in expansion of the laser pulse and higher laser output. In experimental conditions of Fig. 4 total pulse duration was 120 ns while that at half-maximum was over 50 ns with the IES. At lower concentration of Xe and NF_3 in the mixture similarly to [12] the pulse durations increase by a factor of 2 and was as long as 200 ns. Therewith maximal output at 351 nm was as high as 0.6 J with laser No. 2. Maximal electrical efficiency (with respect to stored energy) with laser No. 1 was as high as $\eta_0 = 1.6\%$.

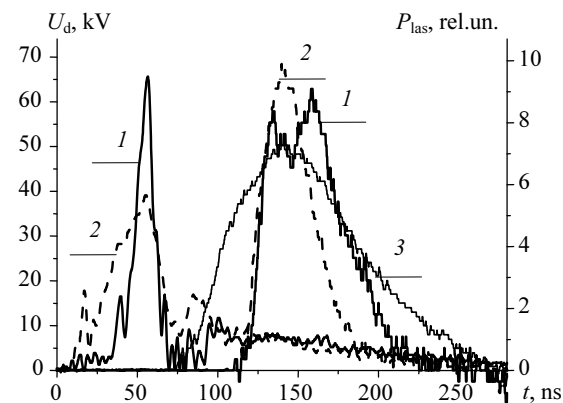


Fig. 4. Waveforms of the voltage across the laser gap U_d and laser pulses P_{las} obtained with IES- (1, 3) and LC-generators (2) in the $Ne:Xe:NF_3 = 2.5$ atm:6:1.5 Torr (1, 2) and $Ne:Xe:NF_3 = 2.5$ atm:3:0.75 Torr (3) mixtures. Laser No. 1, $C_0 = 70$ nF, $U_0 = 30$ kV

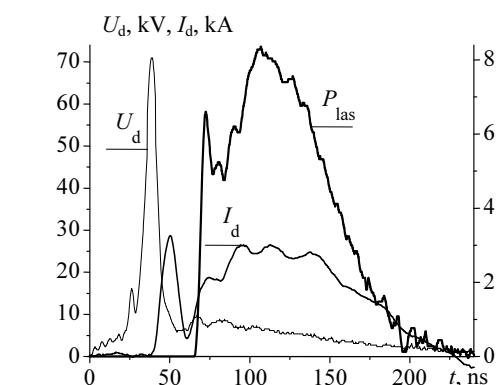


Fig. 5. Waveforms of the voltage across the laser gap U_d , discharge current I_d , and laser pulse at 248 nm P_{las} obtained with the IES-generator in the $Ne:Kr:F_2 = 3$ atm:60:1.5 Torr mixture. Laser No. 1. $C_0 = 70$ nF, $U_0 = 36$ kV

KrF and XeCl lasers. Great discharge improvement and lasing duration extension were also achieved

in the Ne-Xe-HCl and Ne-Kr-F₂ mixtures. Therewith total pulse duration on both XeCl* and KrF* molecules was 160 ns while duration at half-maximum was as long as ~ 100 ns (see Fig. 5). Fig. 6 depicts output and efficiency of XeCl- and KrF-lasers pumped by the IES generator. Laser energy of 1 J with intrinsic efficiency (with respect to deposited energy) up to $\eta_{\text{int}} = 4\%$ was obtained on XeCl* molecules. Up to 650 mJ in a 160 ns pulse was obtained at $\eta = 248 \text{ nm}$. Intrinsic efficiency of the discharge KrF-laser was as high as $\eta_{\text{int}} = 3,3\%$.

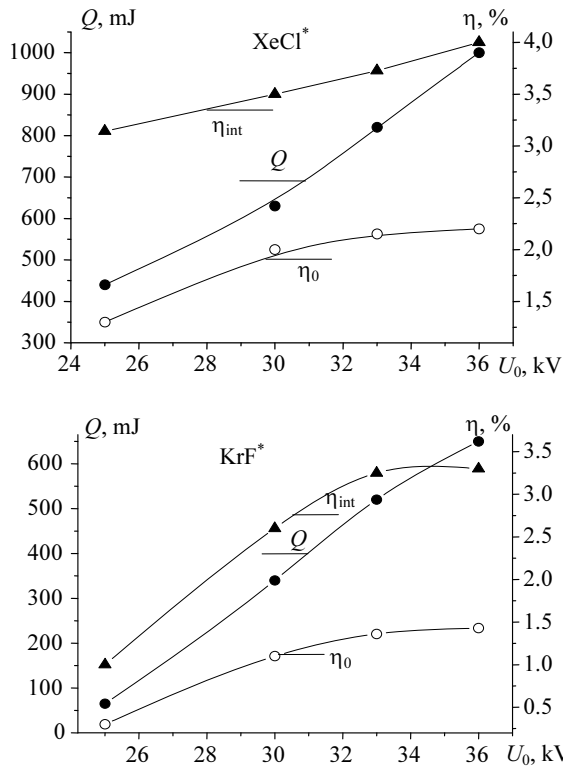


Fig. 6. Output laser energy Q , intrinsic (η_{int}) and electrical (η_0) efficiency of XeCl* and KrF* lasers pumped by the IES as functions of charging voltage of $C_0 = 70 \text{ nF}$. Mixtures of compositions Ne:Xe:HCl = 3.5 atm:24:3 Torr and Ne:Kr:F₂ = 3 atm:60:1.5 Torr are used. Laser No. 1

5. Conclusion

Pre-pulse-sustainer circuit technique on the base of the IES generators was developed for excitation of different gas lasers. It was found that the pre-pulse with

high amplitude and short rise-time along with sharp increase of discharge current significantly improve discharge stability and life-time of the volume discharge in halogen containing gas mixtures. The pre-pulse with high pumping power forms high-density discharge plasma and inversion population in gas mixtures under study within ~ 10 ns and provides both early one-set of lasing and conditions for efficient excitation of an active medium from the storage capacitor.

Long-pulse operation of N₂-, excimer lasers and laser on FI transitions was demonstrated. Maximal at the date output and pulsed power of N₂- and FI-lasers were demonstrated.

UV-laser pulses on XeCl*, XeF* and KrF* molecules with total duration up to 150–200 ns were easily obtained. Maximal output of the excimer lasers was as high as 1 J with the intrinsic efficiency up to 4%.

References

- [1] W.H. Long, J. Plummer, and E.A. Stappaerts, *Appl. Phys. Lett.* **43**, 735 (1983)
- [2] R.S. Taylor and K.E. Leopold, *J. Appl. Phys.* **65**, 22 (1989)
- [3] M.J. Kushner, *IEEE Trans. Plasma Sci.* **19**, 387 (1991).
- [4] E.H. Baksht, A.N. Panchenko, and V.F. Tarasenko, *IEEE J. Quant. Electron.* **35**, 261 (1999).
- [5] Yu.I. Bychkov, E.H. Baksht, A.N. Panchenko, V.F. Tarasenko, S.A. Yampolskaya, and A.G. Yastremsky, *Proc. SPIE* **4747**, 99 (2001).
- [6] E.H. Baksht, A.N. Panchenko, V.F. Tarasenko, T. Matsunaga and T. Goto, *Jap. J. Appl. Phys.* **41**, 3701 (2002).
- [7] I.N. Kononov, A.N. Panchenko, V.F. Tarasenko, and A.E. Tel'minov, *Kvant. Elektron.* **37**, 623 (2007).
- [8] S.N. Buranov, V.V. Gorokhov, V.I. Karelin, and P.B. Repin, *Kvant. Elektron.* **17**, 161 (1990).
- [9] F.E. Sanz and J.M.G. Perez, *Appl. Phys.* **B 52**, 42 (1991).
- [10] P. Parvin, H. Mehravaran, and B. Jaleh, *Appl. Opt.* **40**, 3532 (2001).
- [11] I.J. Bigio and R.F. Begley, *App. Phys. Lett.* **28**, 263 (1976).
- [12] Q.-C. Mei, P.J. M.Peters, M. Trentelman, and W.J. Witteman, *Appl. Phys.* **B 60**, 553 (1995).